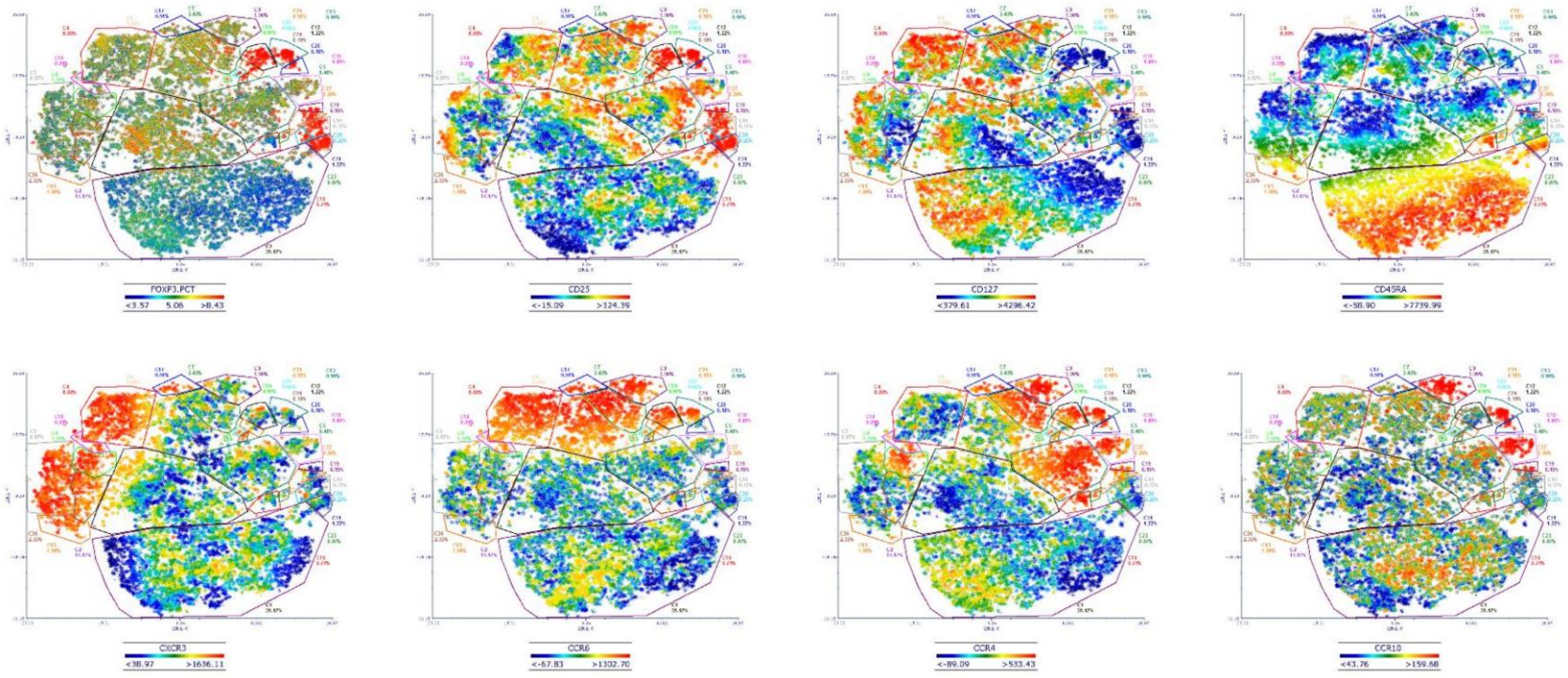

Supplementary Fig. 1 | Fluorescent markers projected across the t-SNE distribution with manual gating (FOXP3, CD25, CD127, CD45RA, CXCR3, CCR6, CCR4, CCR10).

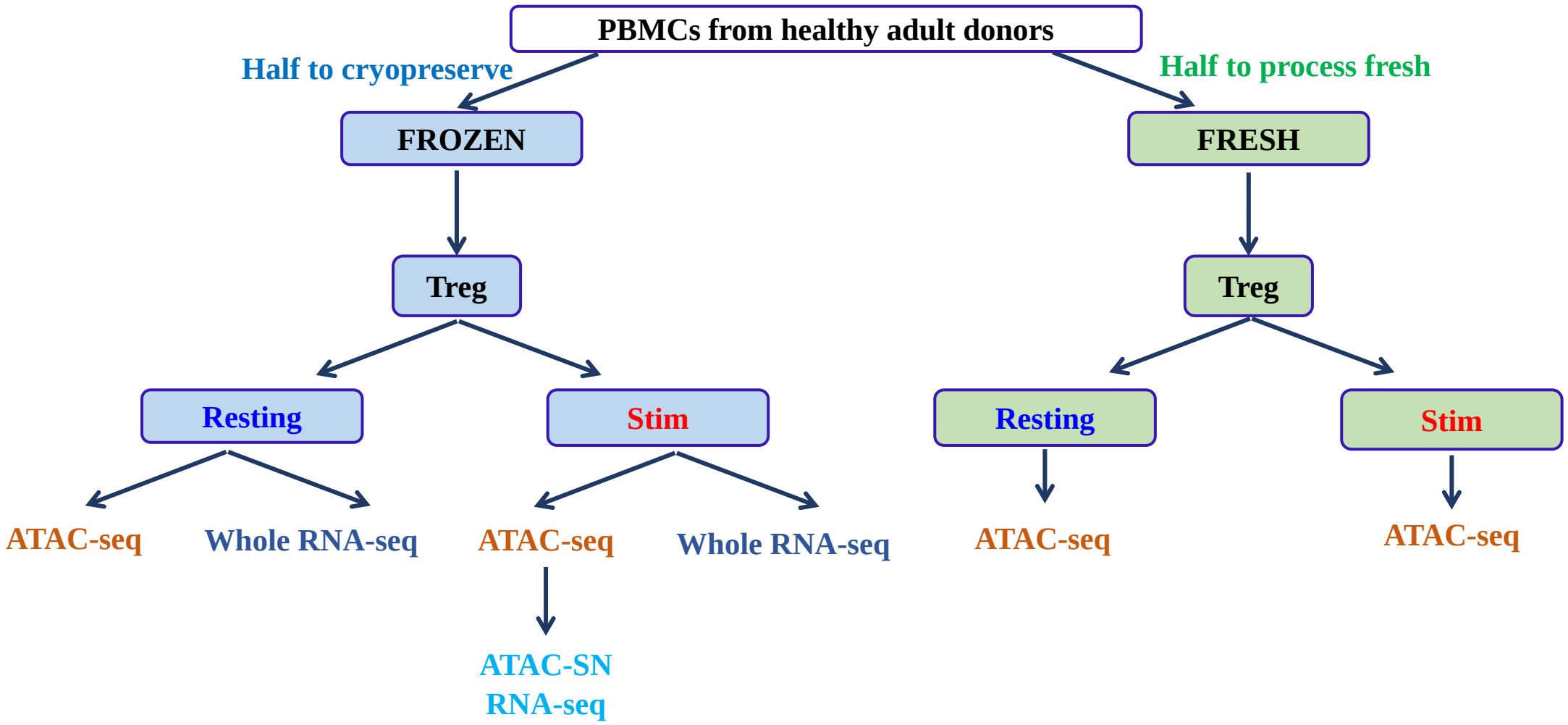

Supplementary Fig. 2 | Workflow of ATAC-seq and RNA-seq library preparation.

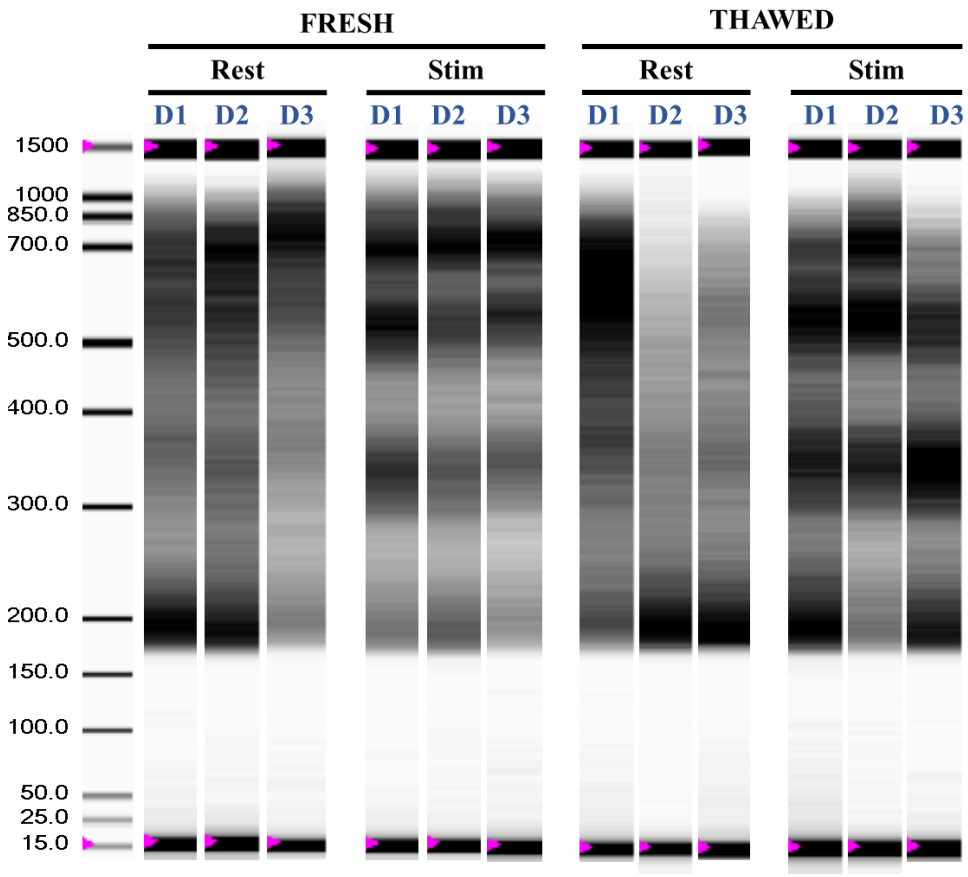

Supplementary Figure. 3 | Virtual gel demonstrating fragment size distribution of amplified fresh and thawed ATAC-seq libraries generated from resting or stimulated Treg cells.

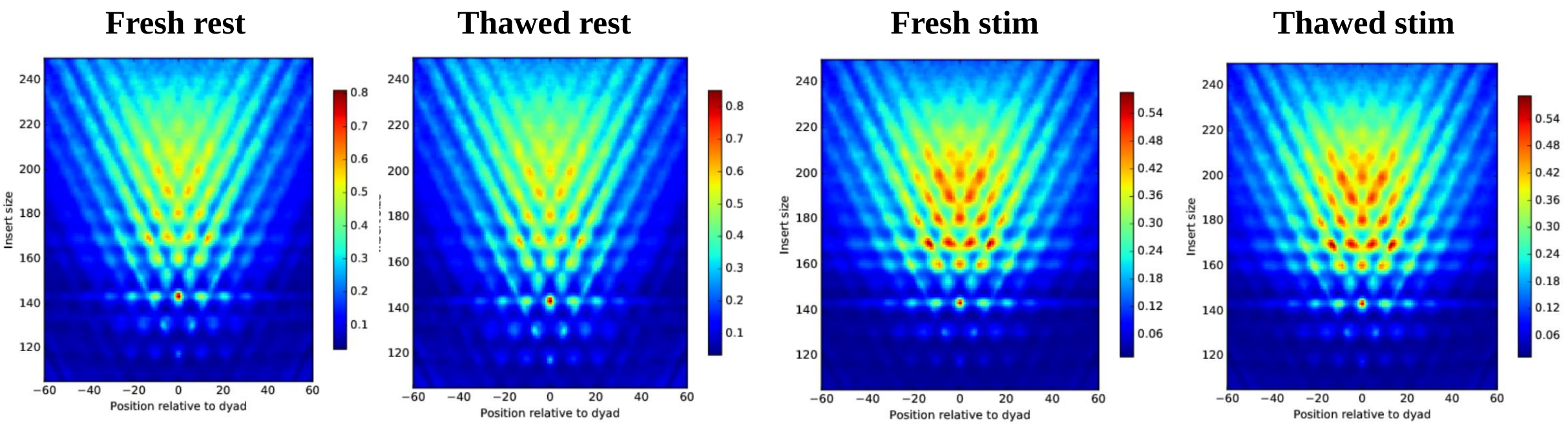

Supplementary Figure. 4 | Biobanking demonstrate structured ATAC-seq signal around nucleosomes. The V-plot maps the density of fragment sizes vs fragment midpoint position relative to nucleosome called by chemical mapping. A highly structured V-pattern observed at fragment sizes spanning a nucleosome for both fresh and thawed Treg cells. 2D nucleosomal "fingerprint" showing ATAC-seq signal around nucleosomes for fresh and thawed Treg cells during resting and stimulated state. V-plot, generated by nucleosome-positioning algorithm, NucleoATAC by Schep, Buenrostro (2015) maps the density of fragment sizes vs fragment midpoint positions relative to nucleosome dyads called by chemical mapping. Y-axis value represents insert size of fragments (bp) and X-axis value represents distance of the fragment midpoint from nucleosomes (bp). These aggregate protection profiles depict a V-shaped structure, where the apex of the "V" represents the smallest possible fragment that spans the DNA protected by a nucleosome. The calculation was performed on pooled sequencing reads representative of 3 adult donors.

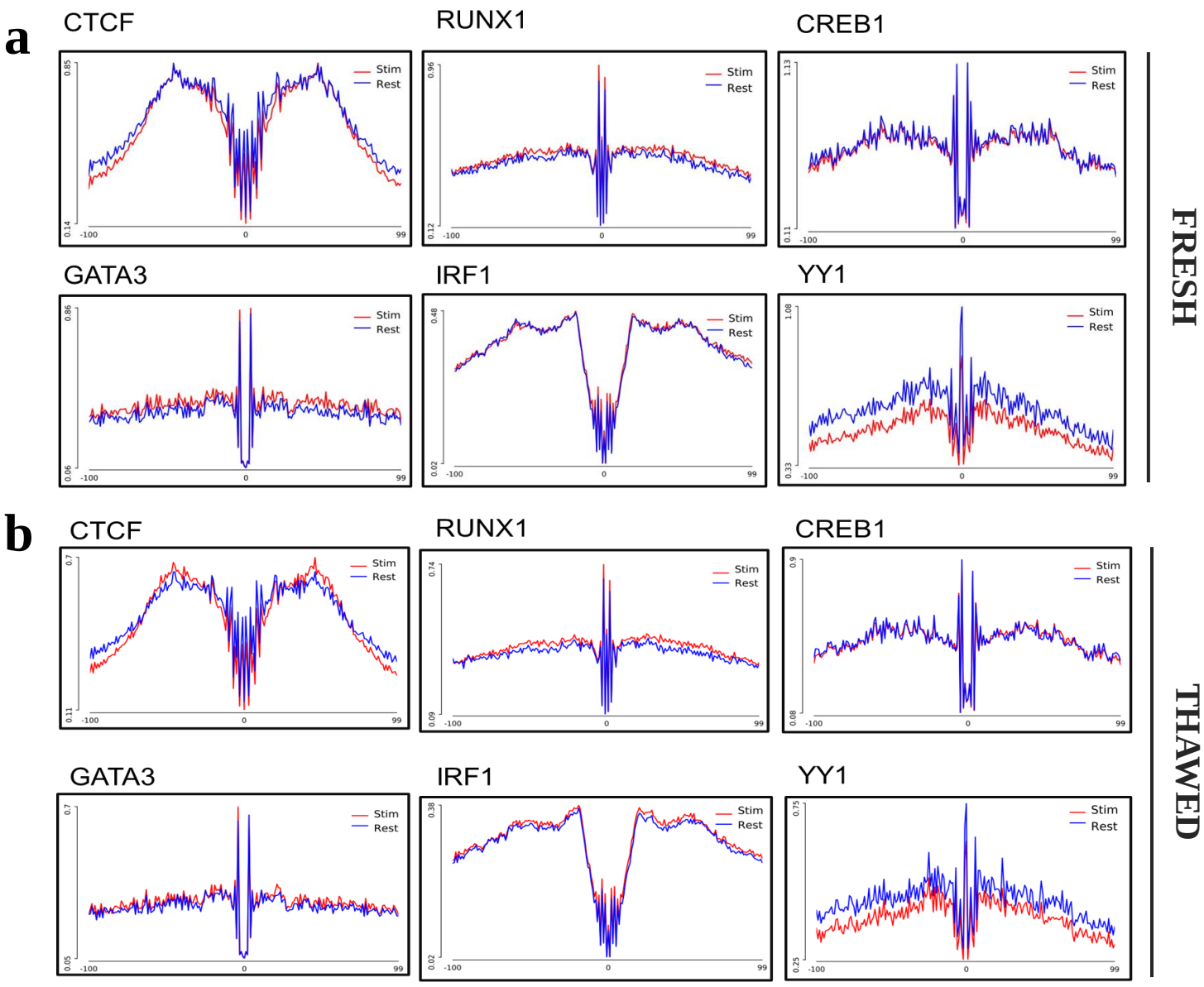

Supplementary Figure. 5 | Thawed Treg cells demonstrate similar responsiveness to stimulation as fresh cells.

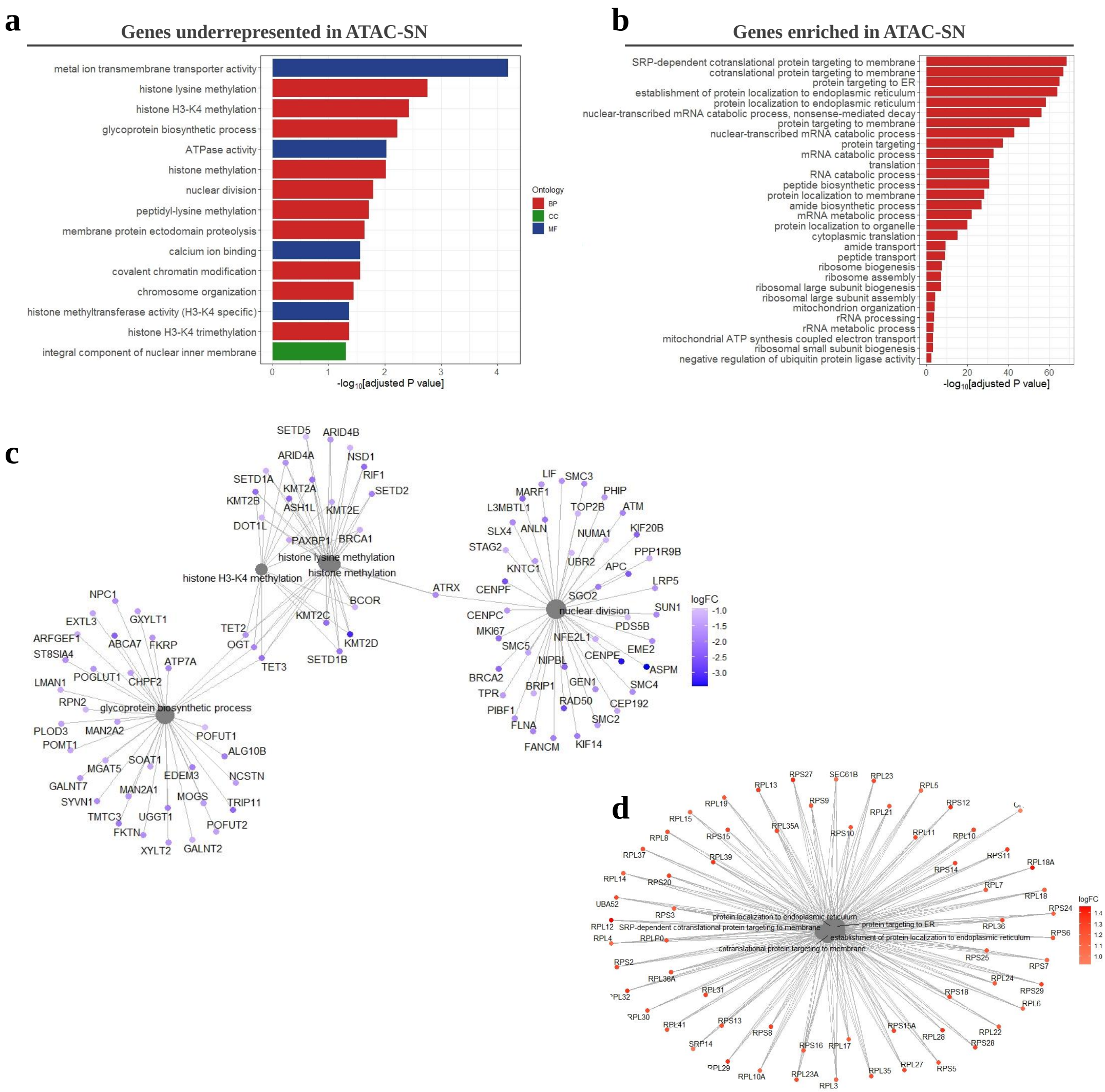

Supplementary Figure. 6 | Differentially expressed genes between ATAC-seq supernatant fraction (ATAC-SN) and whole cells are restricted to subcellular localization mechanism. Gene Ontology (GO) enrichment analyses showing top 30 significantly enriched GO terms associated with genes under-represented (a) or enriched (b) in ATAC-SN. Enrichment plots showing the most significant GO terms and the associated under-represented (c) or enriched (d) genes in ATAC-SN. All GO analyses were performed using a Bonferroni-adjusted p-value < 0.05 as the criteria for significance.

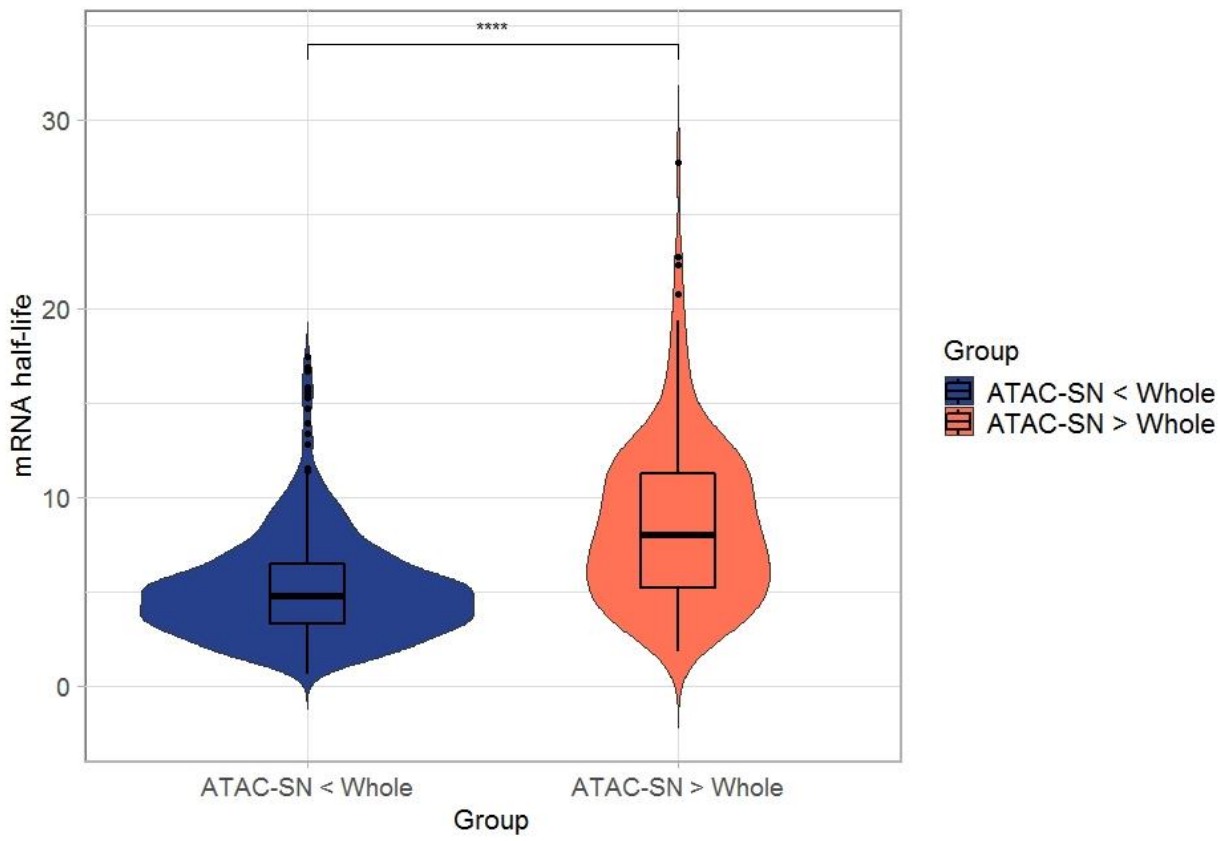

Supplementary Figure. 7 | mRNA half-life of differentially expressed genes between ATAC-SN and whole cell fractions. mRNA half-life data was determined from human HapMap lymphoblastoid cell lines (LCLs), measured as the ratio of nascent RNAs and total RNAs using two-hour 4-thiouridine (4sU) labeling (Duan et al., 2013).

ATAC-SN < Whole, genes detected at a lower level in ATAC-SN than whole cells; ATAC-SN > Whole, genes detected at a higher level in ATAC-SN than whole cells.

a

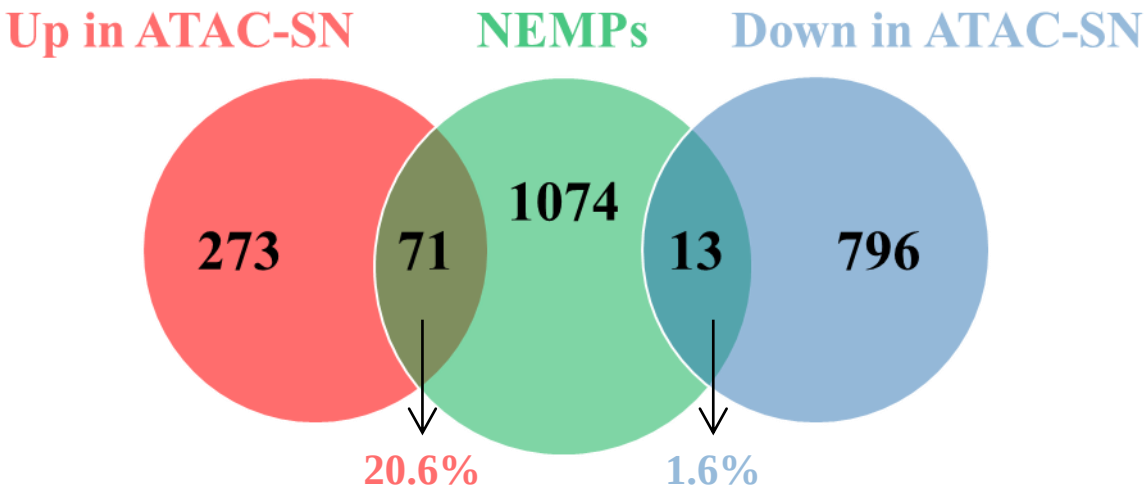

b

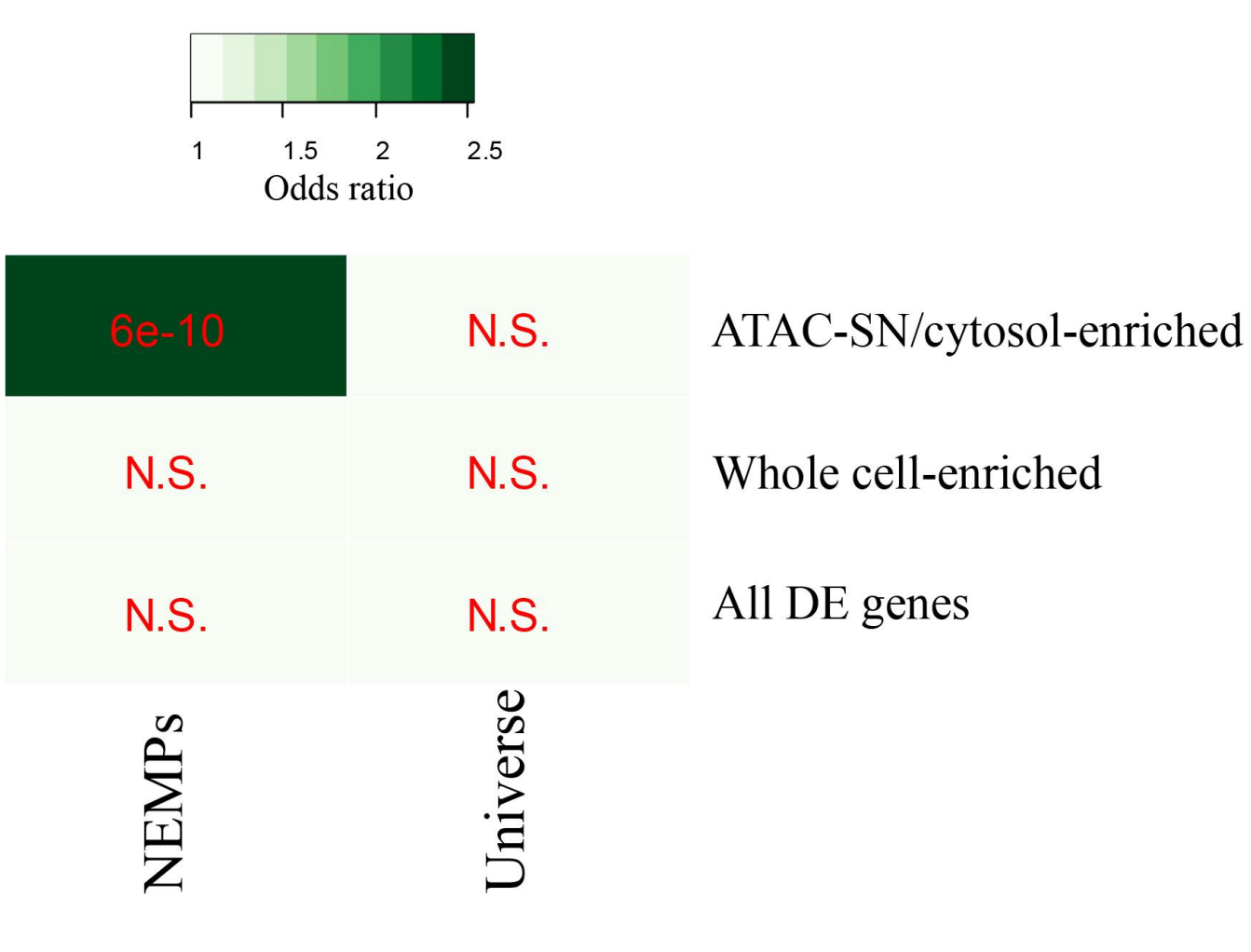

Supplementary Figure. 8 | Gene overlap (a) and Fisher's exact test (b) for assessing the strength of enrichment between genes up- or down-regulated in the ATAC-SN/cytosol fractions and human NEMPs (Nuclear-encoded-mitochondrial proteins). NEMPs database was obtained from the Broad Institute's human MitoCarta2.0 (Calvo et al 2015). These genes (n=1158) encode proteins with evidence for mitochondrial localization. The heatmap color scale represents the odds ratios and the significant p-values, computed from Fisher's exact test, are superimposed on the grids. All DE gene set represents all significantly differentially expressed genes between ATAC-SN and whole cell RNA-seq. Universe gene set contains all genes (DE and non-DE genes) detected in the RNA-seq dataset.

N.S., not significant; DE, differentially expressed.